Journal of the European Ceramic Society 22 (2002) 67–77

www.elsevier.com/locate/jeurceramsoc

Low-temperature fully dense and electrical properties of doped-ZnO varistors by a polymerized complex method

Pedro Durán *, Francisco Capel, Jesús Tartaj, Carlos Moure

Instituto de Cerámica y Vidrio (CSIC), Electroceramics Department, 28500 Arganda del Rey, Madrid, Spain

Received 6 October 2000; received in revised form 16 February 2001; accepted 4 March 2001

Abstract

The preparation of homogeneous and submicrometer doped-ZnO ceramic powders by using a metal-organic polymeric method is described. After calcining and granulating, green compacts with a uniform packing powder and a narrow pore size distribution were achieved. Dense ceramic bodies (>99% theoretical) by normal liquid-phase sintering at temperatures of 850–940°C for 1–5 h were fabricated. It is believed that the low pore-coordination-number allowed a uniform filling of the small pores by the formed liquid in the early stages of sintering and, as a consequence, a high shrinkage rate and rapid densification in a short temperature interval (825–850°C) took place. At those sintering temperatures a small grain growth was produced, and the grain size was maintained below 1 μm. Preliminary electrical results obtained on the doped-ZnO ceramics so fabricated showed nonlinearity coefficients $\alpha \geqslant 70$ and a breakdown voltage V_b (1 mA/cm^2) $\geqslant$ 1500 V/mm.

Keywords: Electrical properties; Powders-chemical preparation; Sintering; Varistors; ZnO

1. Introduction

Electronic circuits and electronic power systems can be subject to several impulse voltage transients generated by lightning, switching and electrostatic discharge accumulated on the human body, therefore, a protection for such devices becomes necessary. Although several kinds of transient suppressers, as for example, silicon carbide and Zener diode can be used, however, the zinc oxide, due to its highly nonohmic behaviour in voltage-current characteristics, is more widely used as a protector in small current electronic circuits as well as for large current transmission lines. ZnO-based varistors contain ZnO as the main component (typically $\geqslant$90%) with several metal oxides (up to 10) added as dopant. Although each additive controls one or several parameters, Bi_2O_3 and Sb_2O_3 can be considered as the most important. For example, Bi_2O_3 plays a significant role in the basic structure of the bulk varistor, Sb_2O_3 enhances its stability, and others like Al_2O_3, MnO, CoO, etc. strongly influence their nonohmic electrical properties. Because of the multi-components present in a ZnO-based varistor, several reactions are to take place during sintering. This leads to a final microstructure, which, in the ideal situation, is constituted on the uniform grain size without porosity, conducting ZnO surrounded by a Bi_2O_3 phase, resulting from the liquid phase at the sintering temperature, segregated at grain boundaries, and homogeneously distributed crystalline secondary phases such as the spinel type $Zn_7Sb_2O_{12}$ and pyrochlore type $Zn_2Bi_3Sb_3O_{14}$. Therefore, the kind, the concentration, and the distribution of both the dopant and the corresponding created phases on sintering, determines the final microstructure and the electrical properties of the obtained varistor material. To fulfil all those specification becomes difficult using the conventional powder preparation method, and albeit the cost of the non-conventional method being quite higher, the advantages of a better chemical homogeneity, a higher powder purity, and a more uniform grain size can decide its use if the final electrical properties are significantly enhanced. In the last decade attempts to achieve this have been carried out.[1–9]

The polymerized route, based on a modification of the Pechini method,[10] was used to prepare doped-ZnO powders which included the four most important Bi, Sb,

* Corresponding author. Tel.: +34-91-8711800; fax: +34-91-8700550.

E-mail address: pduran@icv.csic.es (P. Durán).

0955-2219/01/$ - see front matter
PII: S0955-2219(01)00245-X

Mn, and Co metal oxide additives as raw material for achieving ceramic bodies with controlled microstructure (denoted as unconventional powders). For comparison, a ceramic powder with identical composition, 98 mol% ZnO, 2 mol% ($Bi_2O_3 + CoO + MnO + Sb_2O_3$), was prepared using the conventional mixed oxide method (denoted as conventional powders).

2. Experimental procedure

Doped-ZnO powders were synthesized by the polymerized route as shown in Fig.1. Individual aqueous solutions containing the required amounts of metal nitrates (except in the case of the Sb_2O_3 which was dissolved in melted citric acid) were prepared. Then they were mixed together to produce solutions for gel production. Separately, citric acid (CA) was added to ethylene glycol (EG) in a 1:4 CA/EG molar ratio, and this mixture was stirred at about 80°C to form a transparent solution. The aqueous solution containing only the zinc nitrate was directly mixed with the CA–EG solution. To the resultant transparent solution was then added the aqueous solution containing the Bi, Co, Mn and Sb nitrates, by stirring, and it was heated again at ~90°C for 2 h. The transparent solution was heated at 130°C for the esterification reaction. The temperature was then raised to 180°C by stirring and maintained for 2 h. The resultant concentrated product was used as a precursor for doped-ZnO and calcined at 400°C for 2 h. After calcining, the powder was attrition milled for 4 h in methanol, dried, granulated and then isopressed at 200 MPa. The green compacts were sintered at a constant rate heating (CRH) and cooling (3°C/min) in a dilatometer (Netzsch 402 E of Geratebau, Bayern, Germany) in the temperature range of 850–1200°C for 1–5 h.

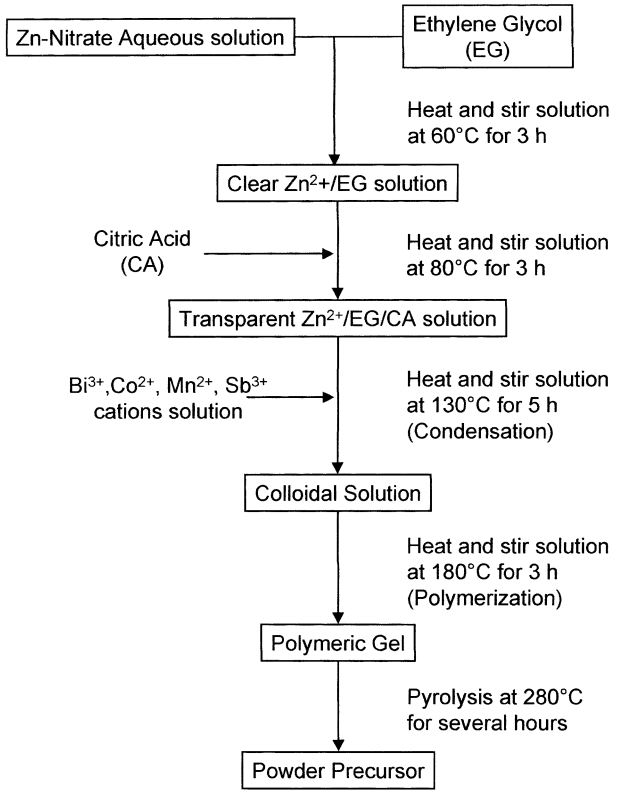

Fig. 1. Flow-chart for preparing doped-ZnO ceramic powders.

The crystallisation process of the polymeric precursors was studied in air by thermogravimetric and differential thermal analysis, (STA 409, Netzsch Geratebau, Selb. Bayern,Germany) using a sample weight of 114 mg and a heating rate of 5°C/min. The existing phases in the sample after calcining were studied by X-ray diffraction (XRD) Cu K_α, 40 KV–40 mA (Siemens D-5000, Erlangen, Germany). The scan rate was 2° 2θ/min for the phase identification. The morphology of the calcined powder was observed using a SEM (Zeiss DSM950, Oberkochem, Germany). Specific surface area of the calcined powders was measured by the single-point BET method (Quantachrome MS-16 model, Suoset, NY). The particle size of the powder was determined by both the crystallite size X-ray diffraction line broadening and from the BET data. Pore size distribution in the green compacts was studied by mercury porosimetry (Micromeritics, Autopore II, 9215, Norgross, USA). Density of the sintered samples was measured by the water immersion method. Microstructure and grain size measurements were carried out on polished and chemically etched surfaces of sintered samples using SEM.

For electrical measurements (with a picoammeter Hewlett-Packard 4140B) a silver paste cured at 60°C was used for the electrodes. The nonohmic property of doped zinc oxide ceramics is described by the empirical relation $J = KV^{\alpha}$, were J and V are the current density and applied field, respectively, and α is called the non-linearity coefficient. It is currently taken as the reciprocal of the slope of the log V versus log J curve. The α value was calculated over the current range, from $\sim 2\times10^{-3}$ to $\sim 12\times10^{-2}$ A/cm^2. The breakdown field V_b (V/mm) was defined as the voltage at the current density of 1 mA/cm^2.

3. Results and discussion

3.1. Powder characterisation

Fig. 2 shows the crystallisation process studied by TG–DTA. It is clearly seen in the TG curve, that with increasing temperature the weight loss increases up to 620°C and beyond that temperature the weight remains constant. Therefore, it can be concluded that at 620°C all the involved reactions in the weight loss process are finished, i.e. the thermal decomposition of all organic products of the precursor (between room temperature

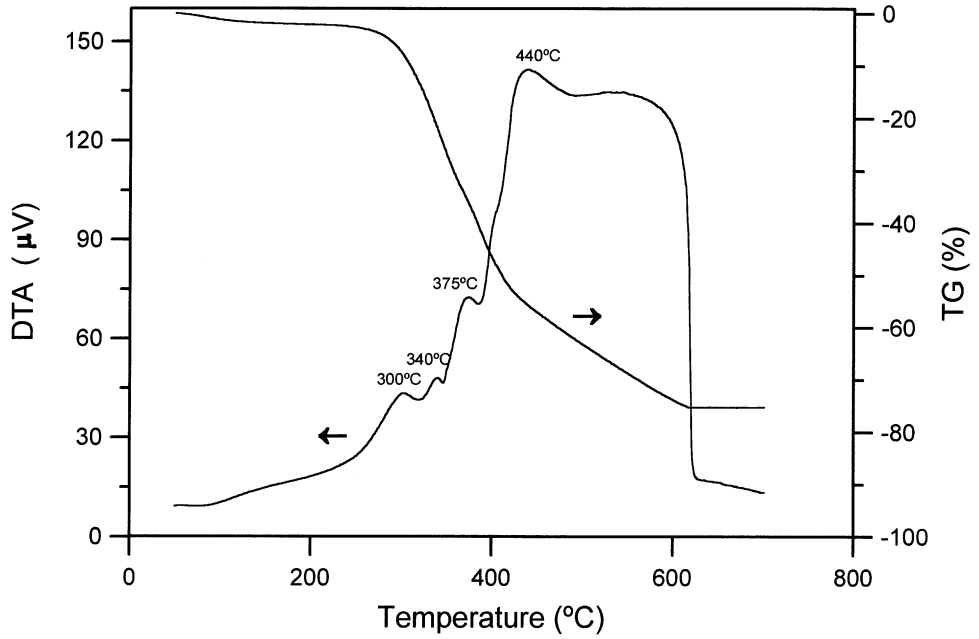

Fig. 2. TG and DTA of (Zn, Bi, Co, Mn, Sb)-citrate polymeric precursor.

and about 400°C), their combustion (from 400 to ~460°C), and the simultaneous crystallisation start of the ZnO zincite structure and, finally, above 480° and up to 620°C, the completion of the crystallisation process. On the other hand, the DTA curve exhibited four exothermal peaks at about 300, 340, 375 and 440°C which correspond well with the above established step reactions.

The resultant products, before calcining at 400°C, were black with a porous structure denoting a high content of organic materials, and after calcining the colour changed to greyish-greenish with a crystallite size of about 28 nm and a specific surface area of 40.4 m^2/g. The polymeric organic precursor showed an expanded and friable structure and the calcined precursor was fine and loose agglomerated, which is a typical characteristic of the powder obtained by this method, see Fig. 3(A) and (B).

Fig. 4 shows the X-ray diffraction spectra with increasing calcination temperature. The dried precursor remained amorphous up to 300°C and, in close agreement with the DTA results (see Fig. 2), then crystallised into a single-phase of ZnO. With increasing temperature, the peaks get sharper and stronger indicating an increase in crystallite size. The presence of the $Zn_7Sb_2O_{12}$ spinel phase or the $Bi_3Zn_2Sb_3O_{14}$ pyrochlore one, if any, were not detected below 700°C. Above that temperature the samples essentially consisted of ZnO as the major phase with a small amount of additional phases which were identified as the mentioned spinel phase and β-Bi_2O_3. The Mn and Co compounds were not detected, probably they have been incorporated into the zincite structure. Similar distribution phases were also found in previous studies on the doped-ZnO system.[1]

3.2. Compaction and sintering

After compaction, the pore size distribution curve showed a quite narrow size distribution with an average pore diameter of 19 nm in the case of the unconventionally prepared powder compacts. By comparison, a wider pore size distribution curve with an average pore diameter of 140 nm for the conventional powder compacts, as shown in Fig. 5 was found. Although a mixture of small and large pores is usually found in a green compact, it is evident from the above results in Figs. 3(B) and 5, that the unconventionally doped-ZnO calcined powders consisted of soft agglomerates which are quite easily broken down during compaction, leading to uniformly packed green compacts. From the almost unimodal pore size distribution curve in these compacts, it is suggested that the methanol milling step was very effective in destroying, if any, the strong agglomerates. On the other hand, the above results confirms the statement that the dried calcined product is a loose powder with a high internal porosity [see Fig. 3(B)], leading to the formation of agglomerates with very low strength. These porous agglomerates, as shown in Fig. 5, can be easily compacted, leading to green compacts in which all the intra-agglomerate pores are of almost identical size. This being so, it is assumed that the particle coordination number will be increased during compaction, and the pore coordination number will be very low.

Fig. 6(A) shows the lineal shrinkage of the two kind of powder compacts during the firing process as studied by CRH dilatometric measurements. The powder compacts prepared by the conventional method show a

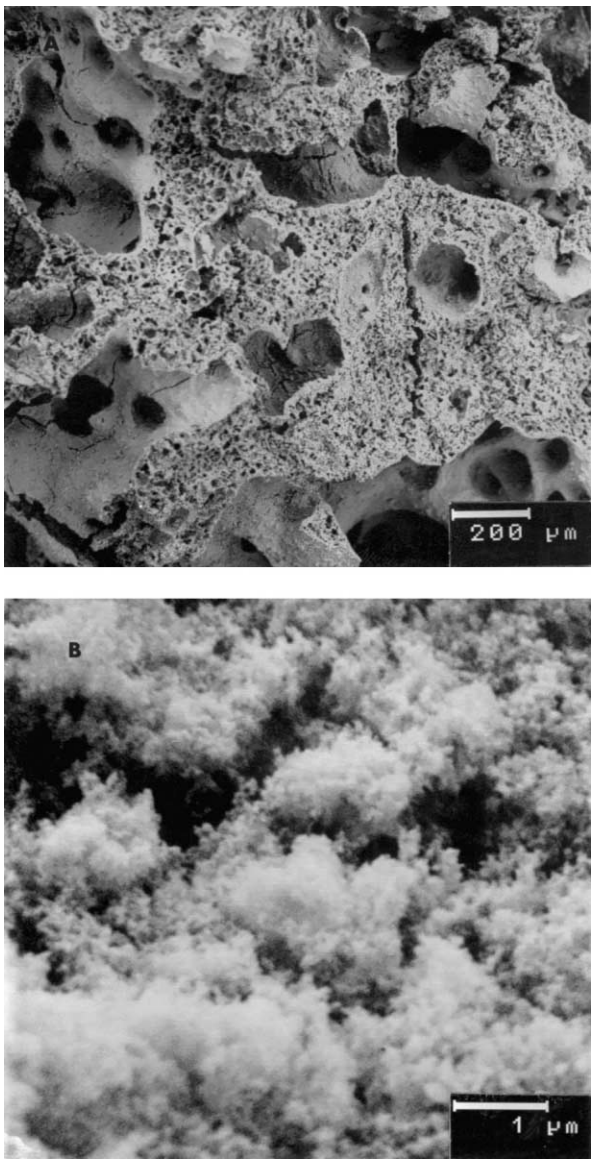

Fig. 3. Morphology of doped-ZnO polymeric resin precursor (A), and (B) after calcining at 400°C.

typical shrinkage curve of solid state reaction sintering with a slow densification rate. The densification rate was sluggish between about 700 and about 1050°C and its final density (~95% theoretical) was not reached up to about 1350°C.

The unconventional doped-ZnO powder compacts yielded a shrinkage curve [see Fig. 6(A)], that shows a regular and rapid densification rate. In this case two maxima on the densification rate curve [see Fig. 6(B)] were produced, which indicates two stages in the sintering process. The first peak, at about 850°C, means liquid-phase sintering with a high densification rate and rapid elimination of the smaller pores.[11] The second one, rather a shoulder, at about 940°C, signifies the elimination of the larger pores and coincides with the end of the densification process, which takes place at about 1000°C. A reduced densification rate occurred in the temperature range 900–1000°C which implies a hindering densification as a consequence of the formation of large pores due to pore coalescence upon sintering. At a temperature slightly above 1000°C fully dense doped-ZnO bodies were achieved by these CRH measurements.

From the above results, it can be concluded that the majority of the pores, i.e. the smaller ones, are eliminated at the lower temperatures (850°C)[12,13] and the larger need higher temperatures to be eliminated. The fast pore elimination at a low-temperature supported the above statement that a high particle coordination number and a uniform packing powder exist in our green compacts. Given that the particle size in the unconventionally prepared doped-ZnO powders is in the nanoscale, a strong capillary pressure and a rapid rearrangement of the solid particles in the liquid is developed as the driving force for the high shrinkage-rate and complete densification[14,15] (see Fig. 6). Although the liquid volume fraction is not very high, a complete liquid phase wetting does occur at the sintering temperature, and the capillary forces from such a wetting contribute to the rapid densification at relatively low temperatures.

In order to study the influence of the heat-treatment on the densification, final microstructure and the electrical properties, we examined samples in which a high-temperature equilibrium microstructure was developed and then were cooled along three different paths.

a. The two kinds of samples (conventional and unconventionally prepared) were heat-treated at 1200°C for 1 h, then rapidly cooled down up to 500°C in the furnace, and then slowly cooled down to room temperature.
b. Unconventionally prepared samples were isothermally densified at 940°C for 1–5 h, then slowly cooled down (3°C/min) to room temperature.
c. Samples unconventionally prepared were fired at 900°C for 5 min, then slowly cooled down up to 850°C, held at this temperature for 1–5 h and then cooled to room temperature at a cooling rate of 3°C/min. This heat-treatment was an attempt to achieve fully dense doped-ZnO without final-stage grain growth.

In the (b) and (c) paths the low density of the conventionally prepared samples precluded its use to compare them with the unconventionally prepared ones. For this reason the conventionally prepared samples were heat-treated up to 1200°C for 2 h, then slowly cooled (2°C/min) down to 720°C, held at this temperature for 2 h and cooled to room temperature.

Fig. 7 shows the relative density vs. sintering time curve and, as can be seen, the conventionally prepared samples do not densify above 96% of theoretical after 5 h at 1040°C. The unconventionally prepared ones were

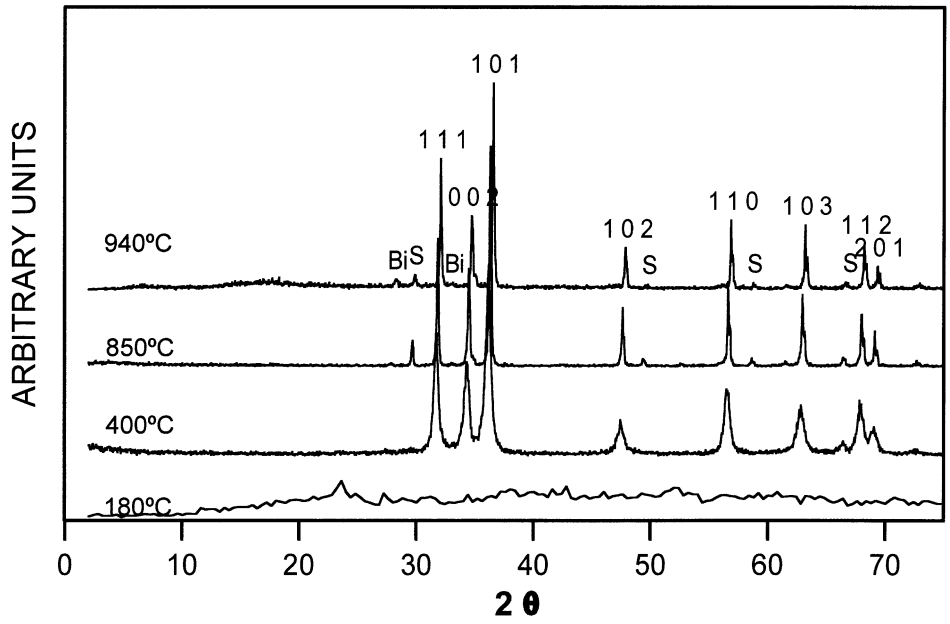

Fig. 4. XRD patterns of the doped-ZnO powders calcined at the indicated temperatures (S) spinel phase, (Bi) β-Bi_2O_3.

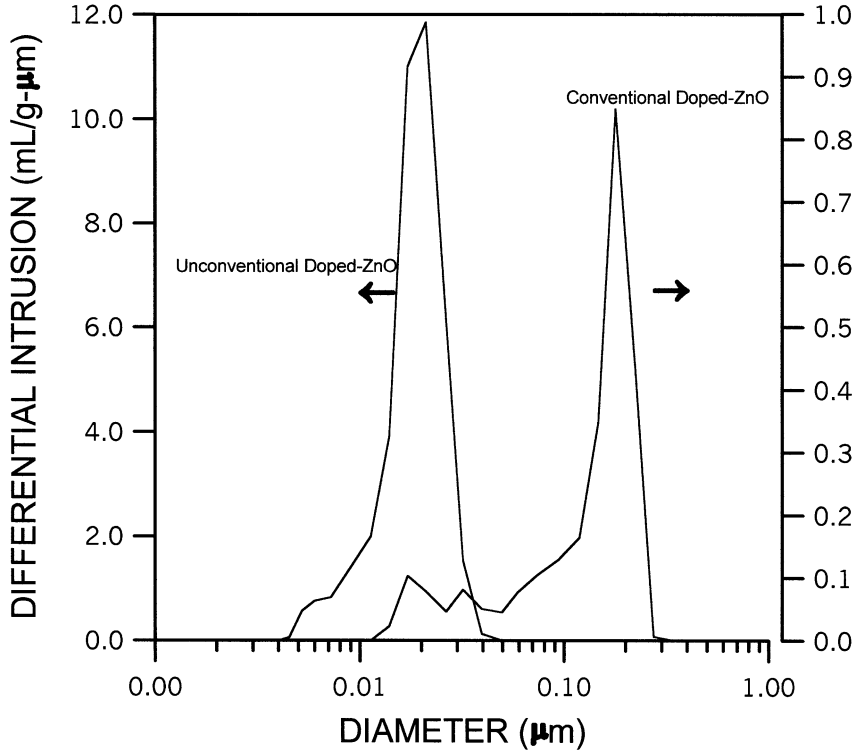

Fig. 5. Pore sizes distribution in green compacts of conventional and unconventionally prepared doped-ZnO powders.

> 98% theoretical after 1 h of heat-treatment at 850°C, and fully dense for a sintering time of 1 and 5 h at 940 and 850°C, respectively. Above that sintering time the density slightly decreased as a consequence, probably, of the grain growth.

From the whole of the above results for the sintering of unconventionally prepared doped-ZnO samples in which the pore size distribution is very narrow, the particle size very uniform and within the nanoscale, we can consider applicable the configuration model of two spheres with a liquid ring at the contact between them,[16,17] in which the force per contact is strongly dependent on the curvature radius of liquid meniscus. The higher the radius of curvature of the liquid meniscus

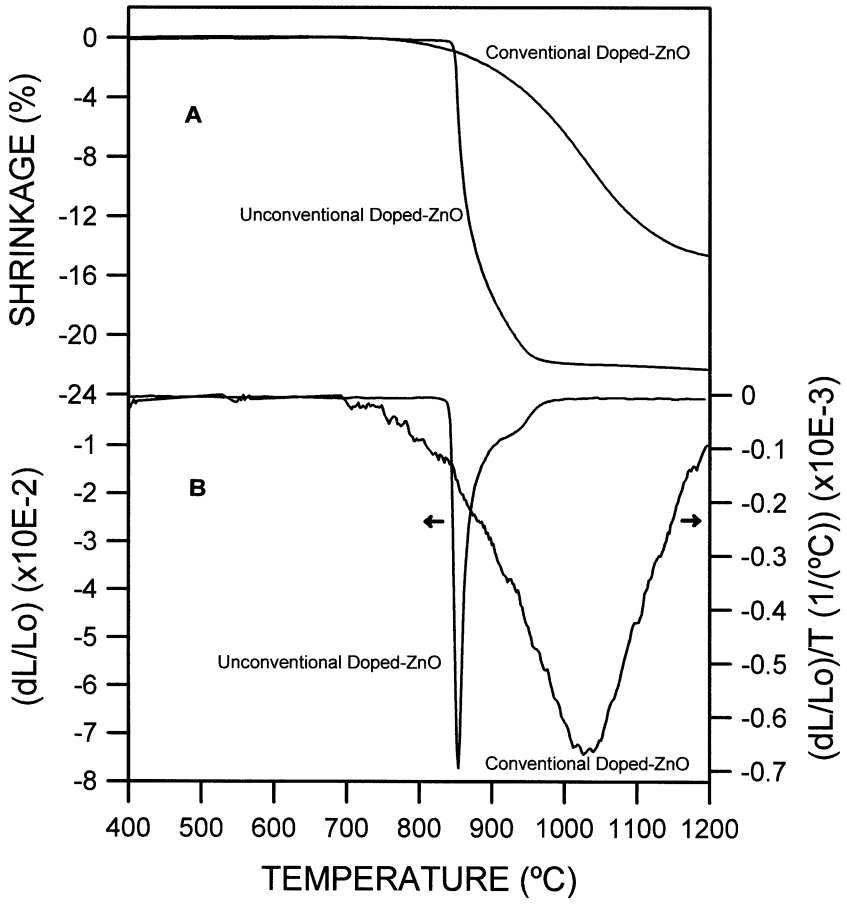

Fig. 6. Shrinkage behaviour of doped-ZnO green compacts during sintering.

the higher is the force per contact and, this being so, the driving force for liquid-phase sintering would depend on the way in which the pores are filled with liquid.[18] On that basis, and taking into account the results in Figs. 5–7, it can be assumed that, although it was not measured, the radius of curvature of the liquid meniscus reached a relatively high value in a short temperature interval (825–850°C) favouring, thus, both the shrinkage rate and densification.

It is believed that just above 740°C, which is the eutectic liquid temperature for the $ZnO–Bi_2O_3$ binary system,[19] a prearrangement of the fine solid particles without or small shrinkage takes place at the beginning of the sintering. As the temperature was increased and with a sufficient amount of liquid-phase, a rapid and uniform homogenisation of the liquid occurred by the effect of the large capillary forces from a wetting liquid which dominates the sintering process at this stage. Since the sintering process is dominated by the elimination of pores, then it must be stated here that a pore filling process has taken place and, as a consequence, a rapid pore elimination via viscous flow mechanism[20] with a sudden density increase occurred in the sintered powder compact [see Figs. 6 and 7]. Therefore, from the above results it can be concluded that by CRH dilatometric measurements, the high densification found in the unconventionally prepared doped-ZnO ceramics up to 850°C, takes place by a rapid rearrangement of nanosized particles associated with easy flow of the liquid. A small grain growth was parallel to the rapid increase of the density with temperature.[14]

3.3. Microstructural development

The microstructure of the samples sintered at 1200°C for 1 h revealed the presence of a phase coming from the solidification of the liquid phase completely wetting like a ring the grain boundaries and grain junctions, [see Fig. 8(A) and (B)]. Of particular interest was the multiple grain junctions, where the liquid and another phase had developed in sufficient amounts to be resolved by the SEM. Fig. 9(A) shows the backscattered image of liquid region in a sample etched with dilute perchloric acid ($HClO_4$) along with the characteristic EDX spectra of the individual present phases. EDX analysis [Fig. 9(B)] revealed that at least three different phases were present in the samples after sintering. The most abundant was ZnO, which appeared like polygonal or rounded grains

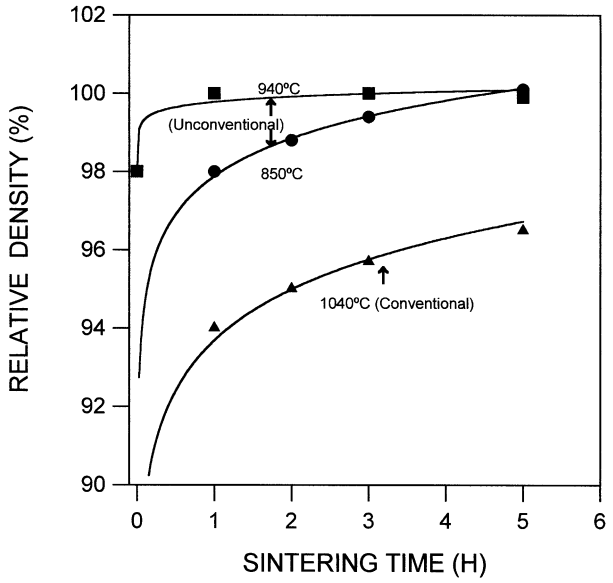

Fig. 7. Isothermal sintering of conventionally prepared doped-ZnO (1040°C), and unconventionally ones (850 and 940°C).

(labelled a) throughout the bulk of the solid matrix. EDX analysis revealed that this phase contained a very small amount of Co. A second phase with a grey colour and surrounded by the liquid (labelled b) can be easily distinguished from the other phases present in the global microstructure. EDX analysis revealed that this phase contained significant amounts of Zn and Sb as well as very small amounts of Co and Mn. Bi was not detected at this phase. The liquid phase (labelled c) was extremely rich in Bi, according to the EDX analysis, and contained a relatively small amount of Zn. The composition of this intergranular phase was 28% ZnO, 72% Bi_2O_3. At these firing conditions no change on cooling, if any, in the dihedral angle of the intergranular liquid-phase took place.

Fig. 10(A)–(F) shows the developed microstructure in the conventionally prepared samples heat-treated at 1200°C for 2 h and in the two kind of unconventionally prepared samples heat-treated at 850 and 940°C and slowly cooled (3°C/min) to room temperature. In this case a liquid phase recession phenomenon has taken place at the same time as a strong change in the dihedral angle of the intergranular liquid phase, so that the second phase no longer penetrates between grain-boundaries after cooling, being preponderantly located at the triple-point junctions. Therefore, it could be said that the increase in the dihedral angle of the multigrain junctions phase in the ceramic microstructure is, thus, a heat-treatment dependent function. Using the line intercept method[21] the average grain size was measured. The grain size was higher than 10 μm for the conventionally prepared samples and between about 1 and 2.5 μm for the unconventionally prepared ones, as shown in Table 1.

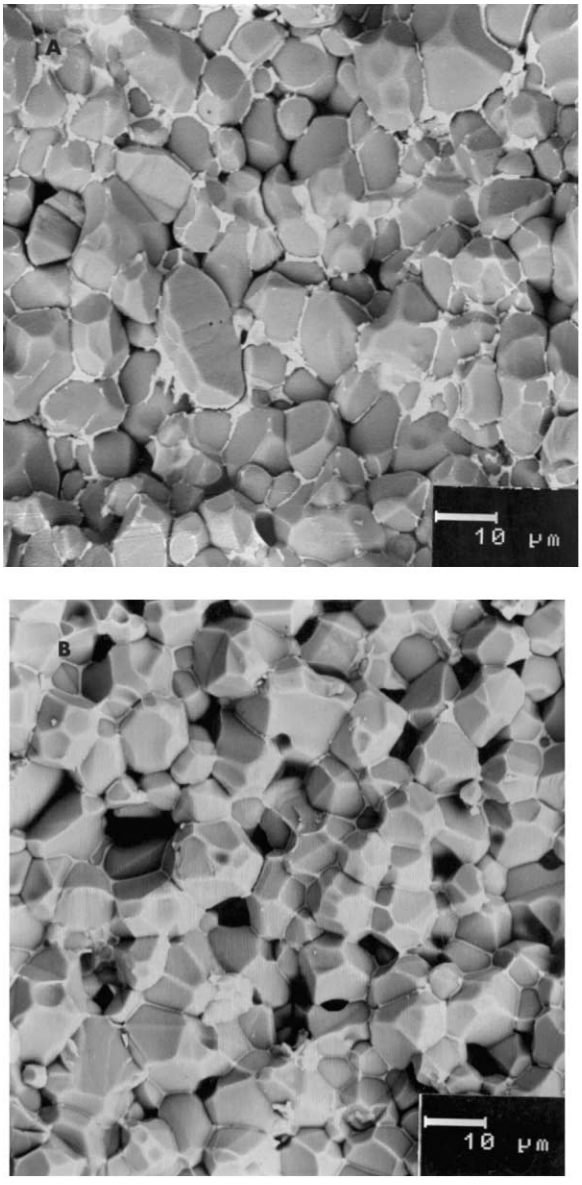

Fig. 8. Developed microstructure on sintering at 1200°C for 1 h and rapidly cooled dawn, (A) conventionally and (B) unconventionally prepared doped-ZnO ceramics.

Although small particles will exhibit a high solubility in a liquid during sintering, giving rise to rapid coarsening by a solution-precipitation mechanism,[14] the small grain growth observed in the sintered samples [see Fig. 10(B)–(F)] indicates that at this temperature, (a) the dissolution rate of the ultrafine ZnO particles in the formed liquid is reasonably low, and (b) as a consequence, the viscosity of the wetting liquid will also be low. In this situation the wetting liquid on cooling rapidly pulls the grain boundaries outward to the triple-point junctions, thus, increasing both the density and the dihedral angle of the liquid menisci between the grains, i.e. most of the ZnO grains will be in direct

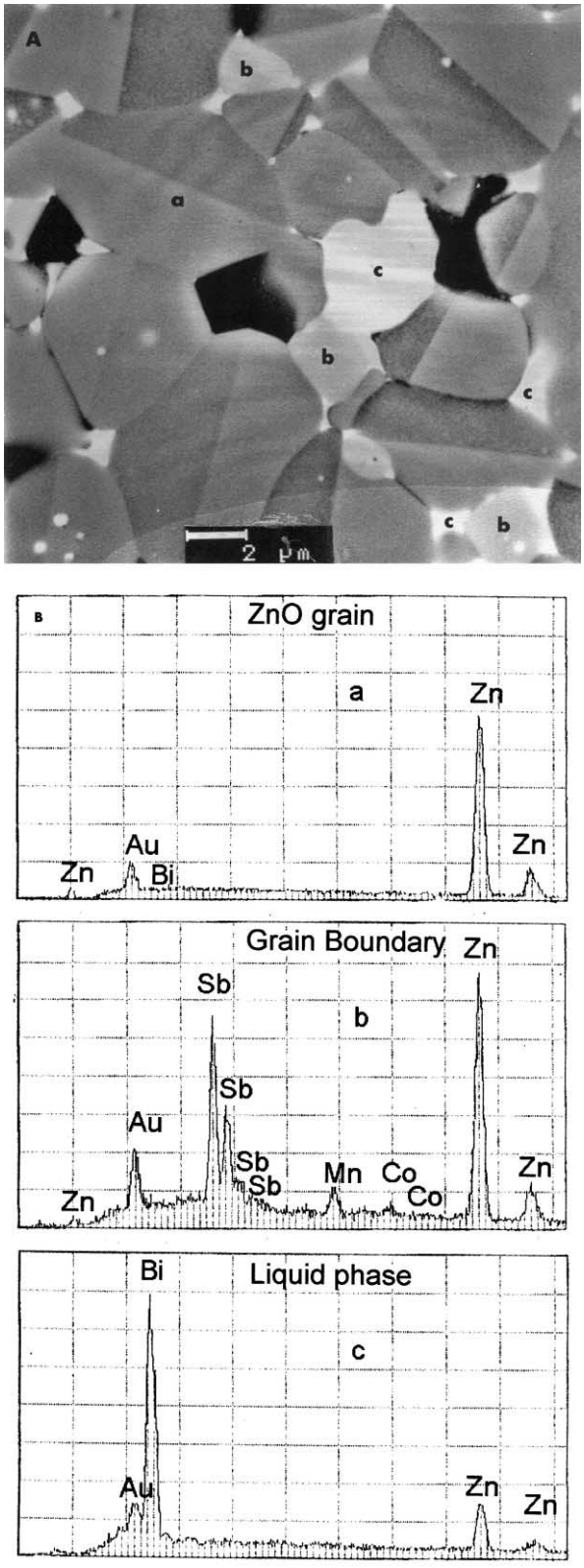

Fig. 9. SEM backscattered image of a sample region showing the morphology of the present phases (A) along with its EDX spectra (B).

contact. For the present samples, in which the volume fraction of the liquid is small and the particle size is also very small (initial size 28 nm, final size < 1 μm), the average liquid layer surrounding a particle, if any, would be very thin, see [Fig. 10].

Research on grain growth during sintering for nanoparticles is lacking, and each of the events present in the liquid-phase sintering, i.e. wetting, rearrangement, and solution-precipitation, should be considered with much care. From Fig. 10(B)–(F), it is evident that in all the cases, the grain size increased with sintering time, and this means that during sintering the grain coarsening process is favoured via solution-precipitation, i.e. the viscosity of the liquid-phase was increased as the amount of dissolved ZnO progressed and the dihedral angle of the liquid meniscus became smaller. On cooling, the dihedral angle shifts according to the viscosity of the generated liquid during sintering, giving rise to the development of microstructures such as those shown in Fig. 10.

3.4. Electrical properties

Preliminary results of electrical measurements indicated that the non-linear coefficients are strongly influenced by the processing method. The advantages of the uniform microstructure in the unconventionally prepared samples were evidenced in the values obtained for the breakdown field V_b and the non-linear coefficient α. When the two kinds of sintered samples are subjected to the same breakdown field V_b, the α value for the unconventionally prepared samples sintered at 940°C was three times higher than for conventionally prepared ones. In some cases, α values as high as 78 and breakdown field V_b (at 1 mA/cm^2) of about 1500 V/mm were measured. Comparatively, α and V_b values as low as 16 and 200 V/mm, respectively, were measured on the conventionally prepared doped-ZnO sintered samples. The high densification level, small grain size, the homogeneous microstructure, and the particular liquid-phase distribution, can be the cause for such a significant difference. Table 1 summarized density, the grain size and the electrical properties for the different doped-ZnO sintered samples.

Since the potential barriers at ZnO–ZnO grain boundaries are the responsible for the nonohmic current-voltage characteristics,[22–25] the results shown in Table 1 are indicating that with increasing sintering time the concentration of dissolved ZnO in the intergranular liquid-phase is also higher and the dihedral angle tends to diminish. Given that in all cases was used the same thermal schedule, i.e. the samples were slowly cooled down then the better performances of the sample heat-treated at 940°C for 0 h are related to the lower fraction of grain boundary area occupied by the liquid-phase, the smaller grain size, and the higher concentration of the direct contact ZnO–ZnO junctions. Such an explanation is consistent with previous suggestions on the effect of liquid-phase on the electrical characteristics of

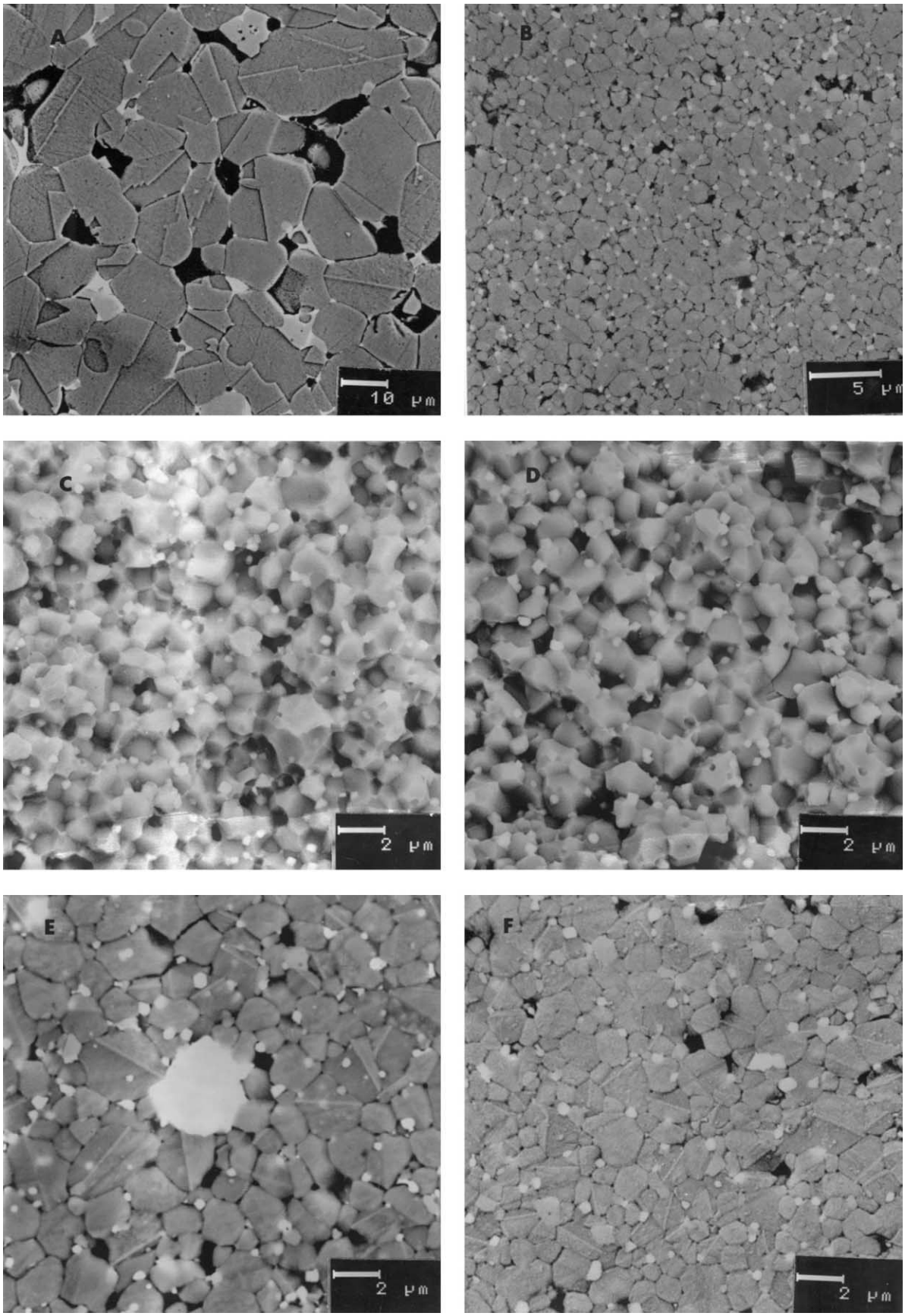

Fig. 10. Microstructures of the conventionally prepared samples (A) sintered at 1200°C and annealed at 720°C, for 2 h, (B)–(D) sintered at 900°C and annealed for 1, 3 and 5 h, (E) sintered at 940°C for 0 h, and (F) sintered at 900°C for 5 min and annealed a 850°C for 5 h.

Table 1
Main characteristics of doped-ZnO ceramics sintered at the indicated temperatures

Samples	Density (% theoretical)	Grain size (μm)	V_b (V/mm)	α
Conventional				
1200°C — 2 h	94	8-10	<200	<16
Unconventional				
1200°C — 1 h	100	8-10	240	26
850°C — 1 h	98	<1	1872	54
850°C — 3 h	>99	1	NM[a]	NM
850°C — 5 h	100	1.5	1766	40
940°C — 0 h	98	0.5	1587	>70
940°C — 1 h	100	0.7	1060	47
940°C — 3 h	100	1.2	NM	NM
940°C — 5 h	99.5	2.2	930	40

[a] NM = not measured.

ZnO varistor.[22,26] On the other hand, similar results also were reported for ZnO–Bi_2O_3 varistors,[24] and for ZnO–Bi–Co ones[25] in which it was considered that both the quality and the quantity of the boundaries in ZnO varistors can strongly influence their nonohmic characteristics. The high V_b and α values measured for the unconventionally prepared doped-ZnO samples confirm the above statement. If this would not be so, then a new approach as would be a grain-boundary solid solution electrical barrier effect should be also taken into account to explain such behaviour. This suggestion would be, on the other hand, consistent with the fact that liquid film-free ZnO grains were found in the microstructure of a zinc oxide varistor.[27–29]

4. Conclusions

Homogeneous and nanosized doped-ZnO ceramic powders were prepared by the metal citrate-based polymeric organic Zn, Co, Mn, Bi, Sb precursor method. After calcining at 400°C the nanosized powders (~28 nm in size) led to green compacts with a very uniform powder packing, a narrow pore size distribution and pore size in the nanoscale (~19 nm), i.e. with a low pore-coordination-number. During sintering it is believed that the formed liquid-phase rapidly filled the small pores, giving rise in a very short temperature interval (between 825 and 850°C) to both a high shrinkage rate and a strong densification with a grain size below 1 μm. Fully dense doped-ZnO ceramic bodies were achieved at 940°C for 1 h. Densification in the two-stage sintering is believed to be based on a rapid rearrangement of the solid nanoparticles in the presence of a liquid-phase at the first stage up to 900°C, and pull outward of the liquid by viscosity decreasing on cooling at 850°C improving ZnO–ZnO direct contacts and suppressing, thus, the grain-boundary migration while keeping grain-boundary diffusion very active to densify. The nonohmic characteristics of such dense ceramics were, in some cases, as high as 78 for the no linear coefficient α, and a breakdown field V_b (at 1 m A/cm^2) of about 1500 V/mm. Values of $\alpha \geqslant 50$ and $V_b \geqslant 1000$ V/mm were currently measured. Comparatively, conventionally prepared samples showed an α and V_b values as low as 16 and 200 V/mm, respectively. It is believed that the high electrical performances of the unconventionally prepared doped-ZnO ceramics can be attributed to a liquid-phase recession phenomenon from the grain boundaries to the multigrain ZnO junctions increasing, thus the ZnO–ZnO direct contacts and the potential barriers effect.

Acknowledgements

The present work was supported by the Spanish CICYT MAT 97-0679-C02-01.

References

1. Matsuoka, M., Progress in research and developments of zinc oxide varistors. In *Advances in Ceramics, Vol.1, Grain Boundary Phenomena in Electric Ceramic*, ed. L. M. Levison. American Ceramic Society, Columbus, OH, 1981, pp. 290–308.
2. Lauf, R. J. and Bond, W. D., Fabrication of high field zinc oxide varistors by sol-gel processing. *Am. Ceram. Soc. Bull.*, 1984, **63**(2), 278–281.
3. Sonder, E., Quinby, T. C. and Kinser, D. L., ZnO varistor made from powders produced using a urea process. *Am. Ceram. Soc. Bull.*, 1986, **65**(4), 665–668.
4. Tiffee, E. I. and Seitz, K., Characterisation of varistor-type materials prepared by the evaporative decomposition of solutions technique. *Am. Ceram. Soc. Bull.*, 1987, **66**(9), 1384–1388.
5. Dosch, R. G., Tlittle, B. A. and Brooks, R. A., Chemical preparation and properties of high-field zinc oxide varistors. *J. Mater. Res.*, 1986, **1**, 90–99.
6. Fan, J. and Sale, F. R., Citrate gel route processing of ZnO varistors. In *British Ceramic Proceeding, Vol. 52, Electroceramics: Production, Properties and Microstructure*, ed. W. E. Lee and A. Bill. The Institute of Materials, London, 1994, pp. 151–157.
7. Hishita, S., Yao, Y. and Shirasaki, S., Zinc oxide varistors made from powders prepared by amine processing. *J. Am. Ceram. Soc.*, 1989, **77**(2), 338–340.
8. Kutty, T. R. and Raghu, N., Characterisation of chemically prepared ZnO powders in relation to the nonlinear resistors. *J. Eur. Ceram. Soc.*, 1993, **11**, 161–170.
9. Simoes, J. A. R., Mantas, P. Q. and Baptista, J. L., Electrical properties of doped ZnO ceramics obtained by controlled chemical synthesis of powders. *Silicat. Ind.*, 1990, **5-6**, 117–120.
10. Pechini, M.P., Method of preparing lead and alkaline earth titanates and niobates and casting methods using the same to form a capacitor. US Patent No 3.330.697, 11 July 1967.
11. Kingery, W. D., Bowen, H. K. and Uhlman, D. R., *Introduction to Ceramics*, 2nd edn. Wiley, New York, 1976 pp. 498-501.
12. Roosen, A. and Hausner, H., Sintering kinetics of ZrO2 powders. In *Advances in Ceramics, Vol. 12*, ed. N. Claussen, M. Ruhle and A. Heuer. The American Ceramics Society, Columbus, OH, 1983, pp. 714–726.

13. Haberco, K., Characteristics and sintering behaviour of zirconia ultra fine powders. *Ceram. Int*., 1979, **5**(4), 148–154.
14. Kingery, W. D., Densification during sintering in the presence of a liquid phase. I. Theory and II. Experimental. *J. Appl. Phys*., 1959, **30**(3), 301–310.
15. Kingery, W. D., Distribution and influence of minor constituents on ceramic formulations. In *Materials Science Research, Vol. 21*, ed. J. A. Pask and A. G. Evans. Plenum Press, New York, 1986, pp. 281–294.
16. Guillespie, T. and Settineri, W. J., The effect of capillary liquid on the force of adhesion between spherical solid particles. *J. Colloid Interface Sci*., 1967, **24**, 199–202.
17. Heady, R. B. and Cahn, J. W., An analysis of the capillary forces in liquid phase sintering of spherical particles. *Metall. Trans*., 1970, **1**, 185.
18. Shaw, T. M., Liquid redistribution during liquid-phase sintering. *J. Am. Ceram. Soc*., 1986, **69**(1), 27–34.
19. Safronov, G. M., Batog, V. N., Stepanyuk, T. V. and Fedorov, P. M. F., Equilibrium diagram of the bismuth oxide-ZnO oxide system. *Russ. J. Inorg. Chem. (Eng. Transl.)*, 1971, **16**(3), 460–461.
20. Eizinger, R., Grain boundary properties in ZnO varistors. In *Advances in Ceramics, Vol. 1, Grain Boundary Phenomena in Electronic Ceramics*, ed. L. M. Levinson. American Ceramics Society, Columbus, OH, 1981, pp. 359–374.
21. Fullman, R. C., Measurement of particle sizes in opaque bodies. *Transmetall. Soc. AIME*, 1952, **197**, 447–452.
22. Philip, H. R., Mahan, G. D. and Levinson, L. M., Schottky barriers in varistors conduction. The need for parallel paths. *Am. Ceram. Soc. Bull*., 1984, **63**(3), 480.
23. Levine, J. D., Theory of varistor electronic properties. *CRC Crit. Rev. Solid State Sci*., 1975, **5**, 597–608.
24. Takemura, T., Kobyashe, M., Takada, Y. and Sato, K., Effects of bismuth sesquioxide on the characteristics of ZnO varistors. *J. Am. Ceram. Soc*., 1986, **69**(5), 430–436.
25. Gambino, J. P., Kingery, W. D., Pike, G. E., Levinson, L. M. and Philipp, H. R., Effect of heat treatments on the wetting behaviour of bismuth-rich intergranular phases in ZnO:Bi:Co varistors. *J. Am. Ceram. Soc*., 1989, **72**(4), 624–645.
26. Baungartner, I. and Einzinger, R., In *Sintering — Theory and Practice*, ed. D. Kolar, S. Pejoonik and M. M. Ristic. Elsevier Scientific, Amsterdam, 1982, pp. 367-371.
27. Morris, W. D., Physical properties of the electrical barriers in varistors. *J. Vac. Sci. Technol*., 1976, **13**(4), 926–931.
28. Clarke, D. R., The microstructural location of the intergranular metal oxide phase in a zinc oxide varistor. *J. Appl. Phys*., 1978, **49**(4), 20407–20411.
29. Clarke, D. R., Grain boundary segregation in a commercial ZnO-based varistor. *J. Appl. Phys*., 1979, **50**(11), 6829–6832.